HHS Public Access

Author manuscript

J Invest Dermatol. Author manuscript; available in PMC 2017 April 04.

Published in final edited form as:

J Invest Dermatol. 2017 March ; 137(3): 631–640. doi:10.1016/j.jid.2016.08.037.

Glycyrrhizin Ameliorates Fibrosis, Vasculopathy, and Inflammation in Animal Models of Systemic Sclerosis

Takashi Yamashita[1], **Yoshihide Asano**[1], **Takashi Taniguchi**[1], **Kouki Nakamura**[1], **Ryosuke Saigusa**[1], **Shunsuke Miura**[1], **Tetsuo Toyama**[1], **Takehiro Takahashi**[1], **Yohei Ichimura**[1], **Ayumi Yoshizaki**[1], **Maria Trojanowska**[2], and **Shinichi Sato**[1]

[1]Department of Dermatology, University of Tokyo Graduate School of Medicine, Tokyo, Japan

[2]Arthritis Center, Boston University School of Medicine, Boston, Massachusetts, USA

Abstract

Systemic sclerosis (SSc) is a multisystem inflammatory and vascular disease resulting in extensive tissue fibrosis. Glycyrrhizin, clinically used for chronic hepatic diseases and itching dermatitis, modulates the pathological processes of inflammation, vasculopathy, and fibrosis in human diseases and their animal models. Therefore, we investigated a potential impact of glycyrrhizin on the key pathological manifestations of SSc, including inflammation, vasculopathy, and tissue fibrosis, with bleomycin-treated mice mimicking the fibrotic and inflammatory components of SSc and endothelial cell-specific *Fli1*-knockout mice recapitulating SSc vasculopathy. Glycyrrhizin significantly ameliorated dermal fibrosis in bleomycin-treated mice, which was partly attributable to blockade of transforming growth factor-β signaling in dermal fibroblasts through the downregulation of thrombospondin 1, a latent transforming growth factor-β receptor, and transcription factors Smad3 and Ets1. Furthermore, bleomycin-dependent induction of T helper type 2-skewed immune polarization, M2 macrophage infiltration, and endothelial-to-mesenchymal transition were greatly suppressed in mice administered glycyrrhizin. Glycyrrhizin also improved vascular permeability of endothelial cell-specific *Fli1*-knockout mice by increasing the expression of molecules regulating vascular integrity. These results indicate that glycyrrhizin ameliorates bleomycin-induced dermal fibrosis through the inhibition of fibroblast activation, T helper type 2-skewed immune polarization, M2 macrophage infiltration, and endothelial-to-mesenchymal transition and improves endothelial Fli1 deficiency-dependent vascular disintegrity, implying its potential as a disease-modifying drug for SSc.

INTRODUCTION

Systemic sclerosis (SSc) is a multisystem connective tissue disease characterized by three cardinal features: immune abnormalities, vasculopathy, and tissue fibrosis (Denton, 2015).

Correspondence: Yoshihide Asano, Department of Dermatology, University of Tokyo Graduate School of Medicine, 7-3-1 Hongo, Bunkyo-ku, Tokyo, 113-8655, Japan. yasano-tky@umin.ac.jp.

CONFLICT OF INTEREST

The authors state no conflict of interest.

SUPPLEMENTARY MATERIAL

Supplementary material is linked to the online version of the paper at www.jidonline.org, and at http://dx.doi.org/10.1016/j.jid.2016.08.037.

Despite an extensive effort to develop new treatments for SSc, the efficacy of any single drug is limited, indicating the importance of combination therapy to control the complicated pathology of this disease. Therefore, it is prudent to take advantage of preexisting anti-fibrotic drugs to explore their potential on the disease course of SSc. Among them, glycyrrhizin is a good candidate because of its wide use for the treatment of liver fibrosis, although its efficacy for SSc-related disorders has not been investigated (Li et al., 2014). To date, glycyrrhizin and its metabolites have been shown to modulate tissue fibrosis, vasculopathy, and inflammation in a variety of human diseases using respective animal models. For instance, glycyrrhizin and its metabolites, such as glycyrrhetinic acid and glycyrrhizic acid, suppress experimental tissue fibrosis of liver and lung by targeting transforming growth factor (TGF)-β signaling and other fibrosis-related pathological events (Gao et al., 2015; Moro et al., 2008). Also, glycyrrhizic acid inhibits angiogenic processes, including migration, invasion, and tube formation, and suppresses production of reactive oxygen species (Kim et al., 2013). Furthermore, glycyrrhizin attenuates pulmonary hypertension and pulmonary vascular remodeling in the monocrotaline-induced rat model of pulmonary arterial hypertension (Yang et al., 2014). Moreover, glycyrrhizin and its metabolites inhibit T helper (Th) type 2 immune response and the inflammatory vascular reaction in various animal models, such as asthma and subarachnoid hemorrhage (Chang et al., 2015; Ma et al., 2013; Sun et al., 2013; Wu et al., 2016). Given that tissue fibrosis, vasculopathy, and inflammation are the three primary pathological components of SSc, glycyrrhizin and its metabolites may have a beneficial disease-modifying effect. To address this issue, we investigated the impact of glycyrrhizin using two complementary animal models of SSc: the bleomycin (BLM)-treated mice mimicking the fibrotic and inflammatory components of SSc (Beyer et al., 2010; Yamamoto, 2006) and the endothelial cell-specific *Fli1*-knockout (*Fli1* ECKO) mice recapitulating SSc vasculopathy (Asano et al., 2010).

RESULTS

Glycyrrhizin alleviates dermal fibrosis in BLM-treated mice

We initially evaluated the effect of glycyrrhizin on BLM-induced dermal fibrosis. In a 4-week injection model, glycyrrhizin significantly decreased dermal thickness in BLM-treated mice and showed no effect on the skin of phosphate buffered saline (PBS)-treated mice (Figure 1a). As well, BLM-dependent decrease in subcutaneous fat thickness, which is generally seen in BLM-treated mice (Marangoni et al., 2015), was significantly attenuated by glycyrrhizin administration (Figure 1a). Consistently, collagen content and the number of myofibroblasts were significantly reduced in BLM-treated mice administered glycyrrhizin compared with those without glycyrrhizin administration (Figure 1b and c). We also assessed whether glycyrrhizin is also effective in therapeutic settings, when treatment is initiated after fibrosis has already been established. To this end, according to previous reports (Huang et al., 2016; Zhang et al., 2015), after completion of the 3-week BLM exposure mice were further subjected to BLM injection for an additional 3 weeks along with the administration of glycyrrhizin or vehicle (PBS). Some mice were treated with PBS alone for 6 weeks or with BLM for 3 weeks, followed by 3 weeks of PBS injections as controls. When dermal thickness was assessed histologically, glycyrrhizin failed to reverse the established skin fibrosis but prevented fibrosis development during the additional 3-week

injection of BLM (see Supplementary Figure S1a online). These findings were confirmed by the measurement of myofibroblasts (see Supplementary Figure S1b). Taken together, these results indicate that glycyrrhizin has a preventive effect, but not a therapeutic effect, on BLM-induced skin fibrosis in mice. In the following experiments, we focused on the mechanism by which glycyrrhizin prevents the development of dermal fibrosis in BLM-treated mice.

To evaluate the effect of glycyrrhizin on the production and the degradation of extracellular matrix, we looked at mRNA levels of the *Col1a1*, *Col1a2*, *Col3a1*, and *Mmp13* genes in the lesional skin of BLM-treated mice. The results showed that *Col1a1*, *Col1a2*, and *Col3a1* mRNA levels were significantly lower, and that *Mmp13* mRNA levels were significantly higher, in BLM-treated mice exposed to glycyrrhizin than in those without glycyrrhizin treatment (Figure 1d). Consistently, matrix metalloproteinase-13 protein expression was increased by glycyrrhizin administration in BLM-treated mice (see Supplementary Figure S2a online). Collectively, these results indicate that glycyrrhizin exerts a potent anti-fibrotic effect on BLM-induced dermal fibrosis by suppressing the production of fibrillar collagens.

Glycyrrhizin inhibits TGF-β–dependent activation of dermal fibroblasts

To investigate the molecular mechanism underlying the anti-fibrotic effect of glycyrrhizin on BLM-induced dermal fibrosis, we examined the expression of growth factors critical for fibroblast activation, such as TGF-β and CTGF. However, glycyrrhizin did not affect *Tgfb1* and *Ctgf* mRNA levels in the skin after 4 weeks of BLM injection (Figure 2a). Because TGF-β is secreted in a latent form by coupling with latency-associated peptide (LAP) and needs to be dissociated from LAP to become biologically active (Lafyatis, 2014; Robertson et al., 2015; Shi et al., 2011), the level of active TGF-β was evaluated by immunostaining for Smad3, indicating canonical TGF-β signaling. BLM-induced nuclear localization of Smad3 was attenuated by glycyrrhizin in dermal fibroblasts (Figure 2b), indicating that TGF-β signaling is suppressed under this condition. Given that TGF-β signaling could be inhibited through extracellular and/or intracellular mechanisms, further analyses were conducted by focusing on these two aspects.

Activation of TGF-β signaling through an extracellular mechanism involves the recruitment of latent TGF-β to LAP receptors on the cell surface followed by the release of active TGF-β from LAP (Lafyatis, 2014; Robertson et al., 2015; Shi et al., 2011). Among cell surface molecules recruiting latent TGF-β by binding with LAP, integrin αVβ3, αVβ5, and TSP-1 are up-regulated on dermal fibroblasts of BLM-treated mice and SSc patients (Lafyatis, 2014; Taniguchi et al., 2015); therefore, we assessed the expression of these molecules in BLM-treated mice. Glycyrrhizin had no effect on the mRNA expression of integrin αV, β3, and β5 subunits; however, it suppressed TSP-1 expression at the mRNA and protein levels in BLM-injected mice (Figure 2c, and see Supplementary Figure S2b), thus raising the possibility that glycyrrhizin may attenuate the establishment of autocrine TGF-β signaling in response to BLM in dermal fibroblasts.

To evaluate the intracellular mechanisms, we used human dermal fibroblasts stimulated with recombinant active TGF-β1, which directly acts on TGF-β receptors. In those cells, glycyrrhizin prevented type I collagen induction by active TGF-β1 (Figure 2d). Under the

same conditions, the expression of Smad3 and Ets1, potent transcriptional activators of the *COL1A1* and *COL1A2* promoters, and the phosphorylation of Smad3 were suppressed, whereas the expression of Fli1, a potent repressor of the *COL1A1* and *COL1A2* promoters, was not affected. Therefore, glycyrrhizin exerts an anti-fibrotic effect on human dermal fibroblasts at least partially by attenuating the TGF-β–dependent induction of Smad3 and Ets1.

Taken together, both extracellular and intracellular mechanisms are likely to contribute to the anti-fibrotic effect of glycyrrhizin on dermal fibroblasts of BLM-treated mice.

Glycyrrhizin alleviates Th2-skewed immune polarization and M2 macrophage infiltration in BLM-treated mice

We next examined the impact of glycyrrhizin on the inflammatory aspects of BLM-treated mice. To this end, we evaluated the expression of proinflammatory and Th cytokines and chemokines, including tumor necrosis factor-α, IL-1β, CCL2, IFN-γ, IL-4, IL-6, IL-10, IL-13, and IL-17A in the skin after 7 days of BLM injection. Among them, a significant reduction by glycyrrhizin was seen in *Il1b*, *Il4*, and *Il6* mRNA levels (Figure 3a). With respect to IL-1β and IL-6, these results were reproduced at the protein level by immunostaining (see Supplementary Figure S3a and b online). Therefore, glycyrrhizin is likely to suppress the proinflammatory and Th2 immune responses in BLM-treated mice. This notion was further confirmed by flow cytometry with lymphocytes isolated from spleen and skin-draining lymph nodes, showing the decreased proportion of IL-4–producing cells among $CD4^+$ T cells, whereas the proportion of IFN-γ– and IL-17A–producing cells was not altered (Figure 3b). Because the proinflammatory and Th2 cytokines are involved in the pathological tissue fibrosis, the reduction of IL-1β, IL-4, and IL-6 partially accounts for the anti-fibrotic effect of glycyrrhizin on BLM-induced dermal fibrosis.

Considering the critical role of M2 macrophages in tissue fibrosis, we also assessed the impact of glycyrrhizin on macrophages in BLM-treated mice. In accordance with its anti-fibrotic property, glycyrrhizin significantly reduced mRNA expression of *Arg1*, an established polarization marker for M2 macrophages, and the number of anginase-1–positive cells in the skin of BLM-treated mice (Figure 3c and d). These results indicate that glycyrrhizin prevents M2 macrophage infiltration, contributing to its anti-fibrotic effect on BLM-induced dermal fibrosis.

Glycyrrhizin abrogates endothelial-to-mesenchymal transition in BLM-treated mice

Endothelial-to-mesenchymal transition (EndoMT) is an important pathological process that contributes to the emergence of activated α-smooth muscle actin (α-SMA)-positive fibroblasts during tissue fibrosis (Jimenez, 2013; Mendoza et al., 2016). Because the number of α-SMA–positive spindle cells was decreased by glycyrrhizin in BLM-treated mice (Figure 1d), we examined whether glycyrrhizin modulates EndoMT by immunostaining for VE-cadherin and FSP-1, markers of endothelial cells and fibroblasts, respectively. Because FSP-1 is also expressed in macrophages and lymphocytes other than fibroblasts under inflammatory conditions (Inoue et al., 2005; Osterreicher et al., 2011; Sun et al., 2015), we regarded fusiform cells as fibroblasts. As already reported, a greater number of spindle-

shaped double-positive cells were observed in the skin after BLM injection (Taniguchi et al., 2015), whereas the number of double positive cells was remarkably decreased by glycyrrhizin administration (Figure 4a). Furthermore, glycyrrhizin decreased the expression of Snail-1, a master regulator of EndoMT, at the mRNA and protein levels in BLM-treated lesional skin (Figure 4b, and see Supplementary Figure S4a online). Relevant to EndoMT, we also evaluated vascular stabilization by assessing the pericyte coverage on blood vessels by immunostaining for α-SMA. As previously reported, pericyte coverage was diminished by BLM injection (Toyama et al., 2016), whereas treatment with glycyrrhizin prevented pericyte loss (Figure 4c), suggesting the stabilization of vasculature by glycyrrhizin. Viewed altogether, these results indicate that glycyrrhizin has beneficial effects on the vasculature by preventing BLM-induced EndoMT and inducing vessel stabilization.

Glycyrrhizin improves the leaky vascular phenotype of *Fli1* ECKO mice

As described above, glycyrrhizin prevented pericyte loss in dermal small vessels of BLM-treated mice. Considering the critical role of pericyte loss for the development of the histological and functional vascular changes characteristic of SSc vasculopathy, such as arteriolar stenosis, capillary dilation, and vascular permeability (Asano and Sato, 2015), glycyrrhizin may exert a disease-modifying effect on SSc vasculopathy by restoring pericyte coverage. To address this issue, we looked at the effect of glycyrrhizin on the vascular phenotype of *Fli1* ECKO mice, which recapitulate SSc vasculopathy because of the loss of pericyte coverage (Asano et al., 2010). Consistent with the results of BLM-treated mice, 2-week administration of glycyrrhizin increased the expression of α-SMA in dermal small vessels of *Fli1* ECKO mice (Figure 5a), indicating the restoration of pericyte coverage. Under the same condition, glycyrrhizin did not affect the abnormal structure of dermal small vessels in *Fli1* ECKO mice (Figure 5b), whereas vascular leakage in dermal small vessels of *Fli1* ECKO mice was improved (Figure 5c). Supporting these findings, the expressions of VE-cadherin, PECAM-1, and PDGF-B, which are the molecules downregulated in dermal small vessels of *Fli1* ECKO mice and related to their vascular disintegrity, were reversed at mRNA levels in the skin of *Fli1* ECKO mice by glycyrrhizin, whereas Fli1 expression was not altered under the same condition (Figure 5d). The increase in VE-cadherin protein expression by glycyrrhizin administration was also confirmed by immunostaining (see Supplementary Figure S4b). Therefore, glycyrrhizin may modulate the pathological vascular changes associated with endothelial Fli1 deficiency, a hallmark of SSc vasculopathy, through a Fli1-independent mechanism.

DISCUSSION

This study was undertaken to evaluate the anti-fibrotic effect of glycyrrhizin on dermal fibrosis in BLM-treated mice, focusing on the principal pathological manifestations of SSc. Glycyrrhizin prevented BLM-induced dermal fibrosis by broadly affecting the pathological processes underlying tissue fibrosis, such as fibroblast activation, Th2-skewed immune polarization, M2 macrophage infiltration, and EndoMT. In addition, glycyrrhizin remarkably improved vascular leakage of *Fli1* ECKO mice. These results indicate that glycyrrhizin has the potential to modulate distinct SSc-related pathologies.

A series of studies using SSc dermal fibroblasts have shown diverse molecular mechanisms underlying the constitutive activation of those cells (Bhattacharyya et al., 2012). Here, we focused on latent TGF-β receptors and transcription factors regulating the *COL1A1* and *COL1A2* promoters. TGF-β is released from cells as a large latent complex consisting of LAP and latent TGF-β–binding proteins, as well as TGF-β itself. TGF-β is initially synthesized as a precursor protein and forms dimers through disulfide bridges. The TGF-β–dimer precursor is cleaved by furin to yield the small latent TGF-β complex, in which LAP and active TGF-β are noncovalently connected. The small latent complex associates with TGF-β–binding proteins through disulfide bonds between LAP and TGF-β–binding proteins, forming the large latent complex. The large latent complex is secreted and incorporated into the extracellular matrix through the interaction of TGF-β–binding proteins with fibrillin-1 and fibronectin. The release of active TGF-β from LAP is regulated by the conformational change or the enzymatic cleavage of LAP (Robertson et al., 2015; Shi et al., 2011). In dermal fibroblasts, this process is at least partially mediated by cell surface LAP receptors, including TSP-1 (Lafyatis, 2014). In the current study, glycyrrhizin suppressed TSP-1 expression, which could result in a reduced activation of latent TGF-β. Glycyrrhizin also abrogated TGF-β–induced Smad3 and Ets1 protein expression, which correlated with the inhibition of collagen production. The inhibitory effects of glycyrrhizin and its metabolites on TGF-β signaling have been reported in other cell types and disease models. Glycyrrhetinic acid, a major metabolite of glycyrrhizin after oral administration, inhibits the nuclear localization of Smad3 in hepatic stellate cells in response to TGF-β stimulation, whereas glycyrrhizin does not affect the expression of type I collagen under the same culture condition (Moro et al., 2008). In addition, glycyrrhizin suppresses carbon tetrachloride-induced liver fibrosis in rats by decreasing Smad2, Smad3, and SP-1 expression (Qu et al., 2015). Furthermore, glycyrrhizic acid, another metabolite of glycyrrhizin, attenuates BLM-induced pulmonary fibrosis in rats through the inhibition of inflammation, oxidative stress, EndoMT, and TGF-β signaling (Gao et al., 2015). Moreover, glycyrrhizic acid inhibits cell proliferation and induces cell cycle arrest and apoptosis in 3T6 fibroblasts (Gao et al., 2015). These previous and current data show that glycyrrhizin and its metabolites exert an anti-fibrotic effect in a cell type- and disease model-specific manners.

The effect of glycyrrhizin on the immune balance of $CD4^+$ T cells has been reported in a murine liver fibrosis model induced by concanavalin A, in which glycyrrhizin suppresses liver fibrosis by shifting the Th1/Th2 and Th17/regulatory T-cell balances, respectively, to a relative dominance of Th1 and regulatory T-cell lineages (Tu et al., 2012). In this study, glycyrrhizin suppressed the expression of IL-4 and IL-6 without affecting the expression of IFN-γ, IL-10, and IL-17A. Furthermore, the number of IL-4–producing $CD4^+$ T cells was decreased, whereas the numbers of IFN-γ– and IL-17A–producing $CD4^+$ T cells were not altered in the BLM model. These results suggest that glycyrrhizin modulates the Th1/Th2 and/or Th17/regulatory T-cell immune balances in a disease model-specific manner. In SSc, Th2/Th17-skewed immune polarization is predominant in the early and fibrotic stage of diffuse subtype, whereas the Th2/Th17 immune response shifts to Th1 immune response in its late stage (Matsushita et al., 2006). SSc fibroblasts are unresponsive to IL-17A, which has an anti-fibrotic effect on dermal fibroblasts, because of the decreased expression of IL-17 receptor A (Nakashima et al., 2012); therefore, the inhibition of Th2 cytokine

production is likely to play an important role in the improvement of tissue fibrosis in SSc. The selective inhibitory effect of glycyrrhizin on the Th2 cytokine production in BLM-treated mice suggests the potential disease-modifying effect of this reagent in SSc.

This study also implied the usefulness of glycyrrhizin for SSc vasculopathy. SSc vasculopathy is pathologically characterized by constitutively activated angiogenesis and EndoMT (Asano and Sato, 2015). In this study, the BLM-dependent induction of the pro-angiogenic status and EndoMT was suppressed by glycyrrhizin, as represented by the decreased expression of α-SMA and the decreased number of double-positive cells for FSP-1 and VE-cadherin, respectively. In addition, as shown in *Fli1* ECKO mice, vascular disintegrity was improved through the increased expression of VE-cadherin, PECAM-1, and PDGF-B by glycyrrhizin. Glycyrrhizin did not affect Fli1 expression during these processes, suggesting that this drug can attenuate vascular symptoms associated with SSc through a Fli1-independent mechanism. Although the detailed mechanism explaining the effect of glycyrrhizin on vasculature still remains unstudied, a possible mechanism is its direct binding to HMGB1, resulting in the inhibition of various biological activities driven by HMGB1 (Musumeci et al., 2014). We recently reported that the activation of Toll-like receptor 4–IFN regulatory factor 5 axis by endogenous ligands, such as HMGB1, plays a pivotal role in vascular destabilization, as represented by the stabilized vasculature in *Irf5*$^{-/-}$ mice treated with BLM (Saigusa et al., 2015). Further studies are under way in our laboratories to confirm this hypothesis.

Recently, we showed that double heterozygous mice for the *Klf5* and *Fli1* genes develop the three cardinal features of SSc: immune activation, vasculopathy, and tissue fibrosis, with the pathological cascade characteristic of this disease (Noda et al., 2014). Supporting the clinical significance of this model, a potential disease-modifying drug against SSc, bosentan, reverses Fli1 expression in various cell types through increasing its protein stability (Akamata et al., 2014, 2015; Saigusa et al., 2016). Because the disease-modifying effect of bosentan is limited (Cutolo et al., 2013; Guiducci et al., 2012; Korn et al., 2004; Matucci-Cerinic et al., 2011), the combination therapy is important to achieve the desirable control of SSc. In this study, we showed that glycyrrhizin did not affect Fli1 expression in dermal fibroblasts stimulated with active TGF-β1. Furthermore, glycyrrhizin improved pathological tissue fibrosis with no effect on the expression levels of integrin αVβ3 and αVβ5, the expressions of which are regulated by Fli1, in BLM-treated mice (Taniguchi et al., 2015). Moreover, the vascular phenotype was normalized by glycyrrhizin without affecting Fli1 expression in *Fli1* ECKO mice. Therefore, the combination therapy of glycyrrhizin with drugs targeting Fli1-dependent disease processes, such as bosentan, may be useful to obtain an additive or synergistic therapeutic effect on SSc.

In summary, this study confirmed the well-known anti-fibrotic effect of glycyrrhizin in the context of BLM-induced dermal fibrosis. A previously unreported finding to our knowledge is the multifaceted inhibitory effect of this reagent on various fibrotic processes associated with SSc. Also, glycyrrhizin improved Fli1 deficiency-associated vasculopathy through a Fli1-independent mechanism. Because glycyrrhizin is already used in clinical practice, the current results suggest that glycyrrhizin warrants evaluation as a disease-modifying agent for SSc.

MATERIALS AND METHODS

Ethics statement

The study was performed according to the Declaration of Helsinki and approved by the ethical committee of The University of Tokyo Graduate School of Medicine. Written informed consent was obtained from healthy donors.

Mice

BLM (Nippon Kayaku, Tokyo, Japan) was dissolved in PBS at a concentration of 1 mg/ml and sterilized by filtration. BLM (200 μg) or PBS was injected subcutaneously into a single location on the shaved backs of C57BL/6 mice (Japan SLC Inc., Tokyo, Japan) with a 27-gauge needle. The injection was carried out daily for 1 week or 4 weeks, depending on the purpose of the experiments. Glycyrrhizin (30 mg/kg; Cokey Systems, Tokyo, Japan) or PBS was intraperitoneally injected. *Fli1* ECKO mice (Asano et al., 2010) (12 weeks old) were intraperitoneally injected with glycyrrhizin (30 mg/kg) or PBS for 2 weeks. All animal protocols were approved by the Animal Care and Use Committee of the University of Tokyo.

Histological assessment and immunostaining

All skin sections were taken from the para-midline, lower-back region. Sections were stained with hematoxylin and eosin. We examined dermal thickness, which was defined as the thickness of skin from the dermal-epidermal junction to the junction between the dermis and subcutaneous fat. The thickness of dermis and subcutaneous fat was measured from seven different randomly selected fields per specimen. Immunohistochemistry was performed using antibodies directed at α-SMA (Sigma-Aldrich, St. Louis, MO), Smad3 (Santa Cruz Biotechnology, Santa Cruz, CA), and arginase-1 (Santa Cruz Biotechnology). For immunofluorescence, goat anti-VE-cadherin antibody (Santa Cruz Biotechnology) and rabbit anti-FSP-1 antibody (Abcam, Cambridge, UK) were used as primary antibodies, and FITC-conjugated donkey anti-rabbit IgG antibody (Santa Cruz Biotechnology) and Alexa Fluor donkey 555 anti-goat IgG antibody (Invitrogen, Carlsbad, CA) were used as secondary antibodies. Coverslips were mounted by using Vectashield with DAPI (Vector Laboratories, Burlingame, CA), and staining was examined by using Bio Zero BZ-8000 (Keyence, Osaka, Japan) at 495 nm (green), 565 nm (red), and 400 nm (blue). All sections were examined independently by two investigators in a blinded manner.

Determination of hydroxyproline content in skin tissue

Following instructions of the QuickZyme Total Collagen Assay kit (QuickZyme Biosciences, Leiden, The Netherlands), 6-mm punch biopsy skin samples were hydrolyzed with 6N HCl, and collagen content was quantified.

Quantitative real-time reverse transcription–PCR

Total RNA was isolated from the skin or cultivated cells with RNeasy spin columns (Qiagen, Crawley, UK). One μg of total RNA from each sample was reverse-transcribed into cDNA using the iScript cDNA synthesis kit (Bio-Rad, Hercules, CA). Gene expression levels were

determined by quantitative real-time reverse transcription–PCR using Fast SYBR Green PCR Master Mix (Applied Biosystems, Carlsbad, CA) on ABI prism 7000 (Applied Biosystems) in triplicates. mRNA levels of target genes were normalized to those of the *Gapdh* gene by the $2^{-\Delta\Delta Ct}$ method. The sequences of primers were summarized in Supplementary Table S1 online.

Flow cytometric analysis

Mice were treated with BLM for 7 days in the presence or absence of glycyrrhizin. The next day, lymphocytes from spleen and skin-draining lymph nodes were obtained. In the surface staining experiments, cells were stained with antibodies against CD19, CD3, and CD4 (all from BioLegend, San Diego, CA). In intracellular cytokine staining, they were stimulated with 10 ng/ml phorbol myristate acetate and 1 μg/ml ionomycin (both from Sigma-Aldrich) in the presence of 1 μg/ml brefeldin A (BD PharMingen, San Diego, CA) for 4 hours. Cells were washed, stained for CD4, treated with fixative/permeabilization buffer (BD PharMingen), and then stained with anti-IL-4, anti-IL-17A, and anti-IFN-γ (all from BioLegend) antibodies. Cells were analyzed on a FACSVerse flow cytometer (BD Biosciences, San Jose, CA). The populations of positive and negative cells were determined using nonreactive isotype-matched antibodies as controls.

Immunoblotting

Human dermal fibroblasts were obtained by skin biopsy from the dorsal forearm of 5 healthy donors. Fibroblasts were cultured in DMEM (Life Technologies, Carlsbad, CA) with 10% fetal calf serum (BioWest, Nuaillé, France), 2 mmol/L L-glutamine (Life Technologies), and the antibiotic antimycotic solution (Sigma-Aldrich). These cells were individually maintained as monolayers at 37 °C in 95% air/5% CO_2. All studies used cells from passage numbers 3–6. Cells were cultured to confluence and then were serum-starved for 24 hours to remove the stimulatory effect of serum. After that, cells were stimulated with TGF-β1 (R&D Systems, Minneapolis, MN) in the presence or absence of glycyrrhizin for 24 hours. Whole-cell lysates were prepared with lysis buffer (1% Triton X-100 [Sigma-Aldrich] in 50 mmol/L Tris-HCl [Sigma-Aldrich], pH 7.4, 150 mmol/L NaCl [Wako, Tokyo, Japan], 3 mmol/L $MgCl_2$ [Wako], and 1 mmol/L $CaCl_2$ [Wako] containing 0.5% Protease Inhibitor Cocktail Set III [Calbiochem, La Jolla, CA]). The samples were run immediately onto NuPAGE Novex 4–12% Bis-Tris gel (Life Technologies) and transferred to nitrocellulose membranes (BIO-RAD, Hercules, CA). The membranes were immunoblotted with antibodies against type I procollagen (Abcam), Smad3 (Santa Cruz Biotechnology), p-Smad3 (Ser423/425; Cell Signaling Technology, Danvers, MA), Ets1 (Santa Cruz Biotechnology), Fli1 (Santa Cruz Biotechnology), and β-actin (Santa Cruz Biotechnology). Bands were detected using enhanced chemiluminescent techniques (Thermo Scientific, Rockford, IL).

Statistical analysis

Statistical analysis was done with one-way analysis of variance followed by Tukey post hoc test for multiple comparison and Mann-Whitney *U* test to compare the distributions of two unmatched groups. Statistical significance was defined as a *P*-value of less than 0.05.

Supplementary Material

Refer to Web version on PubMed Central for supplementary material.

Acknowledgments

Research funding was provided by Cokey Systems. We thank A. Hatsuta, N. Toda, and T. Kaga for tissue processing and staining and E. Numasaki, H. Inomata, S. Itakura, and N. Watanabe for technical assistance. This work was supported by a grant for Research on Intractable Diseases from the Ministry of Health, Labor, and Welfare of Japan.

Abbreviations

α-SMA	α-smooth muscle actin
BLM	bleomycin
EndoMT	endothelial-to-mesenchymal transition
Fli1 ECKO mice	endothelial cell-specific Fli1 knockout mice
FSP-1	fibroblast-specific protein-1
LAP	latency-associated peptide
PBS	phosphate buffered saline
SSc	systemic sclerosis
TGF	transforming growth factor
Th	T helper
VE-Cadherin	vascular endothelial cadherin

References

Akamata K, Asano Y, Aozasa N, Noda S, Taniguchi T, Takahashi T, et al. Bosentan reverses the pro-fibrotic phenotype of systemic sclerosis dermal fibroblasts via increasing DNA binding ability of transcription factor Fli1. Arthritis Res Ther. 2014; 16:R86. [PubMed: 24708674]

Akamata K, Asano Y, Yamashita T, Noda S, Taniguchi T, Takahashi T, et al. Endothelin receptor blockade ameliorates vascular fragility in endothelial cell-specific Fli-1-knockout mice by increasing Fli-1 DNA binding ability. Arthritis Rheumatol. 2015; 67:1335–44. [PubMed: 25707716]

Asano Y, Sato S. Vasculopathy in scleroderma. Semin Immunopathol. 2015; 37:489–500. [PubMed: 26152638]

Asano Y, Stawski L, Hant F, Highland K, Silver R, Szalai G, et al. Endothelial Fli1 deficiency impairs vascular homeostasis: a role in scleroderma vasculopathy. Am J Pathol. 2010; 176:1983–98. [PubMed: 20228226]

Beyer C, Schett G, Distler O, Distler JH. Animal models of systemic sclerosis: prospects and limitations. Arthritis Rheum. 2010; 62:2831–44. [PubMed: 20617524]

Bhattacharyya S, Wei J, Varga J. Understanding fibrosis in systemic sclerosis: shifting paradigms, emerging opportunities. Nat Rev Rheumatol. 2012; 8:42–54.

Chang CZ, Wu SC, Kwan AL. Glycyrrhizin attenuates proinflammatory cytokines through a peroxisome proliferator-activated receptor-g-dependent mechanism and experimental vasospasm in a rat model. J Vasc Res. 2015; 52:12–21. [PubMed: 25896311]

Cutolo M, Zampogna G, Vremis L, Smith V, Pizzorni C, Sulli A. Longterm effects of endothelin receptor antagonism on microvascular damage evaluated by nailfold capillaroscopic analysis in systemic sclerosis. J Rheumatol. 2013; 40:40–5. [PubMed: 23118114]

Denton CP. Systemic sclerosis: from pathogenesis to targeted therapy. Clin Exp Rheumatol. 2015; 33:S3–7.

Gao L, Tang H, He H, Liu J, Mao J, Ji H. Glycyrrhizic acid alleviates bleomycin-induced pulmonary fibrosis in rats. Front Pharmacol. 2015; 6:215. [PubMed: 26483688]

Guiducci S, Bellando Randone S, Bruni C, Carnesecchi G, Maresta A, Iannone F. Bosentan fosters microvascular de-remodelling in systemic sclerosis. Clin Rheumatol. 2012; 31:1723–5. [PubMed: 23053682]

Huang J, Beyer C, Palumbo-Zerr K, Zhang Y, Ramming A, Distler A, et al. Nintedanib inhibits fibroblast activation and ameliorates fibrosis in preclinical models of systemic sclerosis. Ann Rheum Dis. 2016; 75:883–90. [PubMed: 25858641]

Inoue T, Plieth D, Venkov CD, Xu C, Neilson EG. Antibodies against macrophages that overlap in specificity with fibroblasts. Kidney Int. 2005; 67:2488–93. [PubMed: 15882296]

Jimenez SA. Role of endothelial to mesenchymal transition in the pathogenesis of the vascular alterations in systemic sclerosis. ISRN Rheumatol. 2013:835948. [PubMed: 24175099]

Kim KJ, Choi JS, Kim KW, Jeong JW. The anti-angiogenic activities of glycyrrhizic acid in tumor progression. Phytother Res. 2013; 7:841–6.

Korn JH, Mayes M, Matucci Cerinic M, Rainisio M, Pope J, Hachulla E, et al. Digital ulcers in systemic sclerosis: prevention by treatment with bosentan, an oral endothelin receptor antagonist. Arthritis Rheum. 2004; 50:3985–93. [PubMed: 15593188]

Lafyatis R. Transforming growth factor b–at the centre of systemic sclerosis. Nat Rev Rheumatol. 2014; 10:706–19. [PubMed: 25136781]

Li JY, Cao HY, Liu P, Cheng GH, Sun MY. Glycyrrhizic acid in the treatment of liver diseases: literature review. Biomed Res Int. 2014; 2014:872139. [PubMed: 24963489]

Ma C, Ma Z, Liao XL, Liu J, Fu Q, Ma S. Immunoregulatory effects of glycyrrhizic acid exerts anti-asthmatic effects via modulation of Th1/Th2 cytokines and enhancement of CD4(+)CD25(+)Foxp3+ regulatory T cells in ovalbumin-sensitized mice. J Ethnopharmacol. 2013; 148:755–62. [PubMed: 23632310]

Marangoni RG, Korman BD, Wei J, Wood TA, Graham LV, Whitfield ML, et al. Myofibroblasts in murine cutaneous fibrosis originate from adiponectin-positive intradermal progenitors. Arthritis Rheumatol. 2015; 67:1062–73. [PubMed: 25504959]

Matsushita T, Hasegawa M, Hamaguchi Y, Takehara K, Sato S. Longitudinal analysis of serum cytokine concentrations in systemic sclerosis: association of interleukin 12 elevation with spontaneous regression of skin sclerosis. J Rheumatol. 2006; 33:275–84. [PubMed: 16465658]

Matucci-Cerinic M, Denton CP, Furst DE, Mayes MD, Hsu VM, Carpentier P, et al. Bosentan treatment of digital ulcers related to systemic sclerosis: results from the RAPIDS-2 randomised, double-blind, placebo-controlled trial. Ann Rheum Dis. 2011; 70:32–8. [PubMed: 20805294]

Mendoza FA, Piera-Velazquez S, Farber JL, Feghali-Bostwick C, Jimenez SA. Endothelial cells expressing endothelial and mesenchymal cell gene products in lung tissue from patients with systemic sclerosis-associated interstitial lung disease. Arthritis Rheumatol. 2016; 68:210–7. [PubMed: 26360820]

Moro T, Shimoyama Y, Kushida M, Hong YY, Nakao S, Higashiyama R, et al. Glycyrrhizin and its metabolite inhibit Smad3-mediated type I collagen gene transcription and suppress experimental murine liver fibrosis. Life Sci. 2008; 83:531–9. [PubMed: 18771671]

Musumeci D, Roviello GN, Montesarchio D. An overview on HMGB1 inhibitors as potential therapeutic agents in HMGB1-related pathologies. Pharmacol Ther. 2014; 141:347–57. [PubMed: 24220159]

Nakashima T, Jinnin M, Yamane K, Honda N, Kajihara I, Makino T, et al. Impaired IL-17 signaling pathway contributes to the increased collagen expression in scleroderma fibroblasts. J Immunol. 2012; 188:3573–83. [PubMed: 22403442]

Noda S, Asano Y, Nishimura S, Taniguchi T, Fujiu K, Manabe I, et al. Simultaneous downregulation of KLF5 and Fli1 is a key feature underlying systemic sclerosis. Nat Commun. 2014; 5:5797. [PubMed: 25504335]

Osterreicher CH, Penz-Osterreicher M, Grivennikov SI, Guma M, Koltsova EK, Datz C, et al. Fibroblast-specific protein 1 identifies an inflammatory subpopulation of macrophages in the liver. Proc Natl Acad Sci USA. 2011; 108:308–13. [PubMed: 21173249]

Qu Y, Zong L, Xu M, Dong Y, Lu L. Effects of 18a-glycyrrhizin on TGF-b1/Smad signaling pathway in rats with carbon tetrachloride-induced liver fibrosis. Int J Clin Exp Pathol. 2015; 8:1292–301. [PubMed: 25973013]

Robertson IB, Horiguchi M, Zilberberg L, Dabovic B, Hadjiolova K, Rifkin DB. Latent TGF-b-binding proteins. Matrix Biol. 2015; 47:44–53. [PubMed: 25960419]

Saigusa R, Asano Y, Taniguchi T, Yamashita T, Ichimura Y, Takahashi T, et al. Multifaceted contribution of the TLR4-activated IRF5 transcription factor in systemic sclerosis. Proc Natl Acad Sci USA. 2015; 112:15136–41. [PubMed: 26598674]

Saigusa R, Asano Y, Yamashita T, Taniguchi T, Takahashi T, Ichimura Y, et al. Fli1 deficiency contributes to the downregulation of endothelial protein C receptor in systemic sclerosis: a possible role in prothrombotic conditions. Br J Dermatol. 2016; 174:338–47. [PubMed: 26399195]

Shi M, Zhu J, Wang R, Chen X, Mi L, Walz T, et al. Latent TGF-b structure and activation. Nature. 2011; 474:343–9. [PubMed: 21677751]

Sun L, Sun C, Liang Z, Li H, Chen L, Luo H, et al. FSP1(+) fibroblast sub-population is essential for the maintenance and regeneration of medullary thymic epithelial cells. Sci Rep. 2015; 5:14871. [PubMed: 26445893]

Sun Q, Wang F, Li W, Hu YC, Li S, Zhu JH, et al. Glycyrrhizic acid confers neuroprotection after subarachnoid hemorrhage via inhibition of high mobility group box-1 protein: a hypothesis for novel therapy of subarachnoid hemorrhage. Med Hypotheses. 2013; 81:681–5. [PubMed: 23932051]

Taniguchi T, Asano Y, Akamata K, Noda S, Takahashi T, Ichimura Y, et al. Fibrosis, vascular activation, and immune abnormalities resembling systemic sclerosis in bleomycin-treated Fli-1-haploinsufficient mice. Arthritis Rheumatol. 2015; 67:517–26. [PubMed: 25385187]

Toyama T, Asano Y, Akamata K, Noda S, Taniguchi T, Takahashi T, et al. Tamibarotene ameliorates bleomycin-induced dermal fibrosis by modulating phenotypes of fibroblasts, endothelial cells, and immune cells. J Invest Dermatol. 2016; 136:387–98. [PubMed: 26967475]

Tu CT, Li J, Wang FP, Li L, Wang JY, Jiang W. Glycyrrhizin regulates $CD4^+$ T cell response during liver fibrogenesis via JNK, ERK and PI3K/AKT pathway. Int Immunopharmacol. 2012; 14:410–21. [PubMed: 22940540]

Wu Q, Tang Y, Hu X, Wang Q, Lei W, Zhou L, et al. Regulation of Th1/Th2 balance through OX40/OX40L signalling by glycyrrhizic acid in a murine model of asthma. Respirology. 2016; 21:102–11. [PubMed: 26467500]

Yamamoto T. The bleomycin-induced scleroderma model: what have we learned for scleroderma pathogenesis? Arch Dermatol Res. 2006; 297:333–44. [PubMed: 16402183]

Yang PS, Kim DH, Lee YJ, Lee SE, Kang WJ, Chang HJ, et al. Glycyrrhizin, inhibitor of high mobility group box-1, attenuates monocrotaline-induced pulmonary hypertension and vascular remodeling in rats. Respir Res. 2014; 15:148. [PubMed: 25420924]

Zhang Y, Dees C, Beyer C, Lin NY, Distler A, Zerr P, et al. Inhibition of casein kinase II reduces TGFb induced fibroblast activation and ameliorates experimental fibrosis. Ann Rheum Dis. 2015; 74:936–43. [PubMed: 24431397]

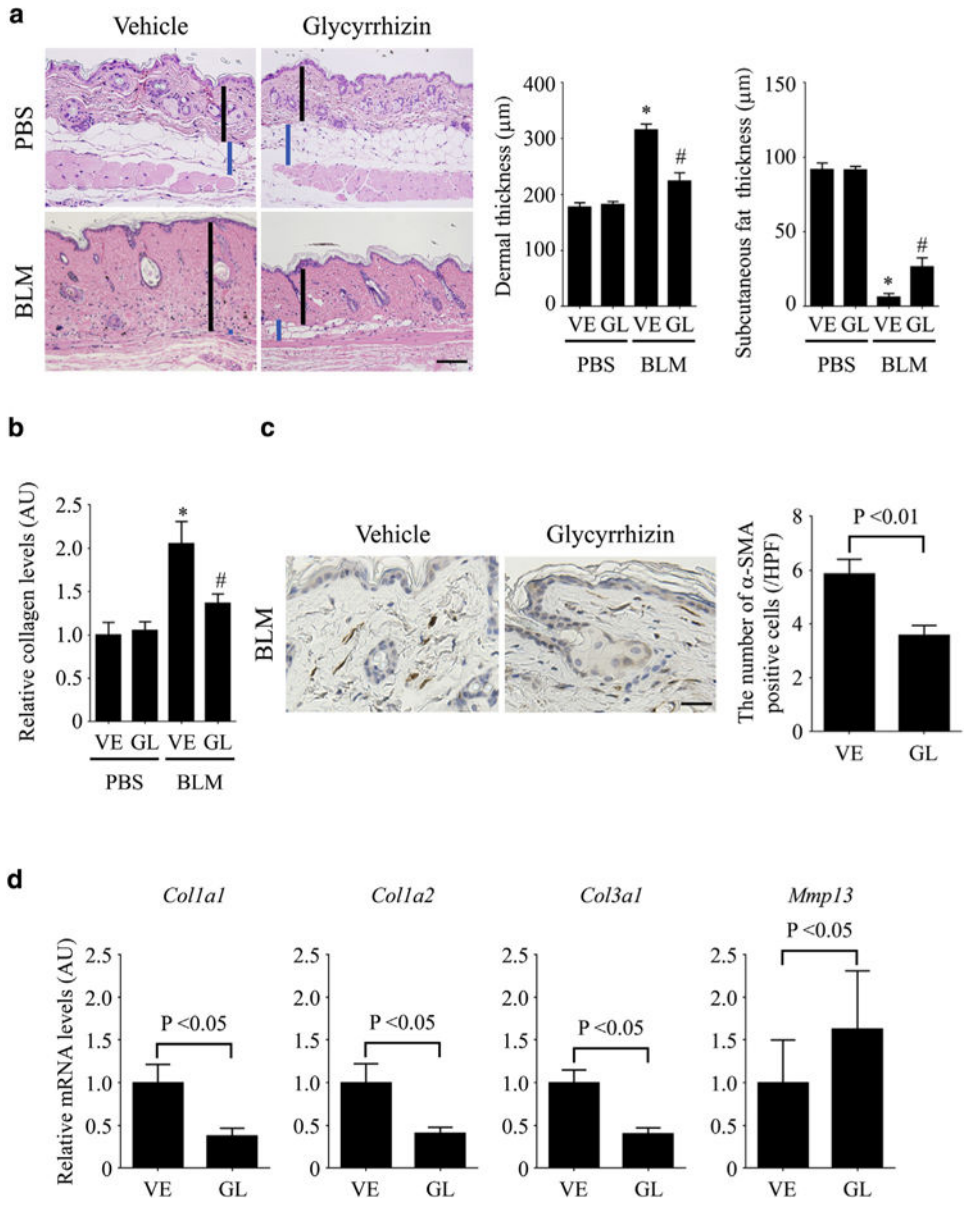

Figure 1. Glycyrrhizin alleviates dermal fibrosis in BLM-treated mice

(**a**) Mice were injected with BLM or PBS along with the administration of glycyrrhizin (GL) or PBS (vehicle [VE]) for 4 weeks. Skin sections were evaluated with hematoxylin and eosin stain. The vertical bars show dermal thickness (black) and subcutaneous fat thickness (blue). Representative images are shown. Original magnification × 100. Data of dermal thickness and subcutaneous fat thickness are summarized as a graph. (**b**) Collagen contents were measured by hydroxyproline assay. (**c**) The number of α-SMA–positive cells was evaluated by immunohistochemistry. (**d**) *Col1a1, Col1a2, Col3a1*, and *Mmp13* mRNAs in the lesional skin were assessed by quantitative real-time reverse transcription–PCR. Each graph indicates mean ± standard error of the mean of the indicated parameters (n = 6–7 per group). Scale bars = 100 μm for **a** and 20 μm for **c**. **P* < 0.05 versus PBS-VE group. #*P* < 0.05 versus

BLM-VE group. α-SMA, α-smooth muscle actin; AU, arbitrary unit; BLM, bleomycin; GL, glycyrrhizin; HPF, high power field; PBS, phosphate buffered saline; VE, vehicle.

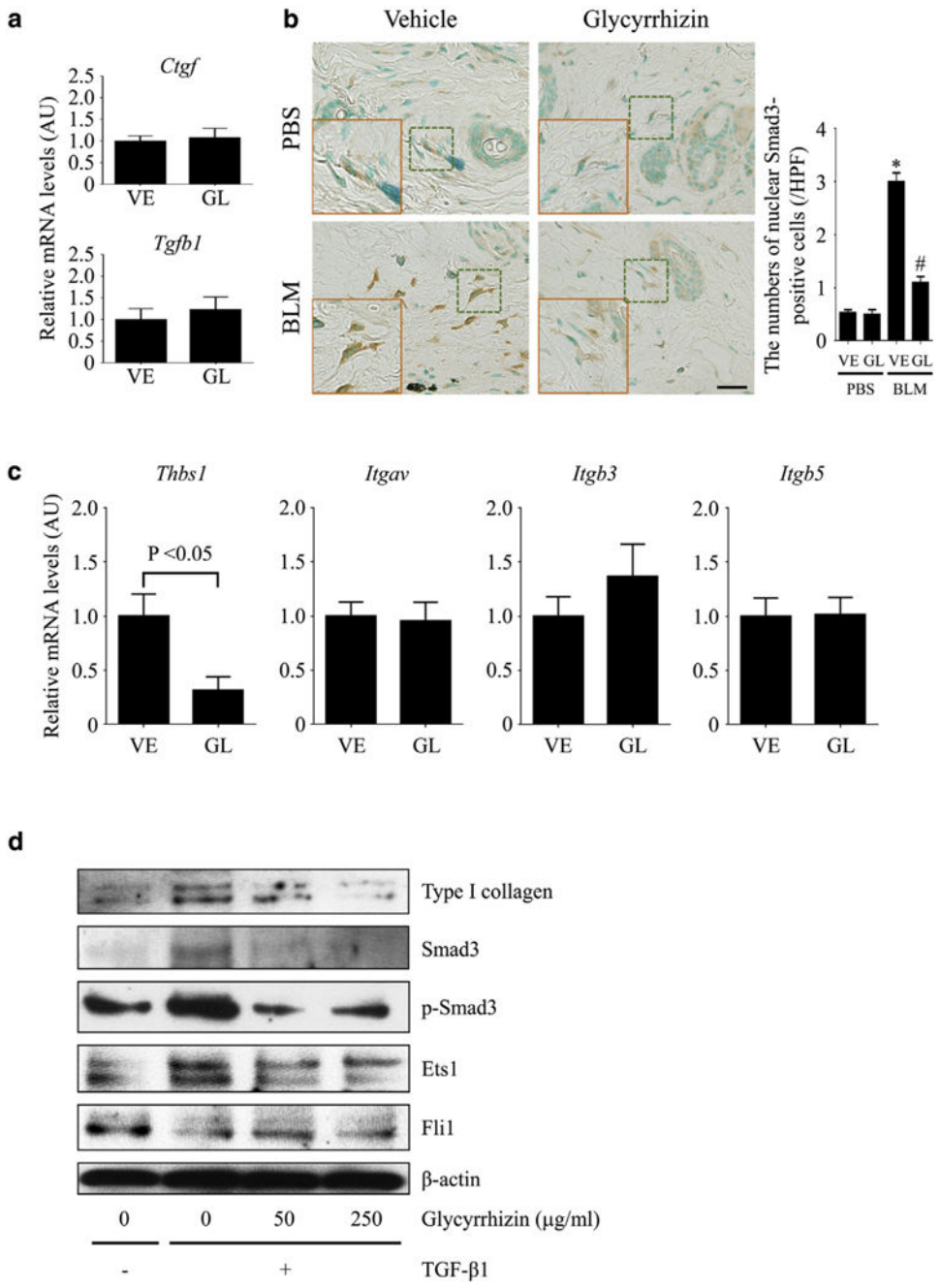

Figure 2. Glycyrrhizin inhibits TGF-β–dependent activation of dermal fibroblasts

(**a**–**c**) Four-week BLM injection was conducted for mice treated with glycyrrhizin (GL) or PBS (vehicle [VE]). (**a**) *Tgfb1* and *Ctgf* mRNAs were assessed by quantitative real-time reverse transcription–PCR in the skin. (**b**) Nuclear Smad3-positive cells were evaluated by immunostaining in the skin. The insets depict representative dermal fibroblasts shown with dotted squares. (**c**) *Thbs1*, *Itgav*, *Itgb3*, and *Itgb5* mRNAs, encoding thrombospondin 1, integrin αV, integrin β3, and integrin β5, were determined by quantitative real-time reverse transcription–PCR in the skin. (**d**) Three strains of human dermal fibroblasts were stimulated with active TGF-β1 for 24 hours in the presence or absence of glycyrrhizin. Type I collagen,

Smad3, Ets1, and Fli1 expression and Smad3 phosphorylation were evaluated by immunoblotting. Representative blots of 3 independent experiments with similar results are shown. Each graph indicates mean ± standard error of the mean of the indicated parameters (n = 6–7 per group). Scale bar = 20 μm. *$P < 0.05$ versus PBS-VE group. $^{\#}P < 0.05$ versus BLM-VE group. AU, arbitrary unit; BLM, bleomycin; GL, glycyrrhizin; HPF, high power field; PBS, phosphate buffered saline; TGF, transforming growth factor; VE, vehicle.

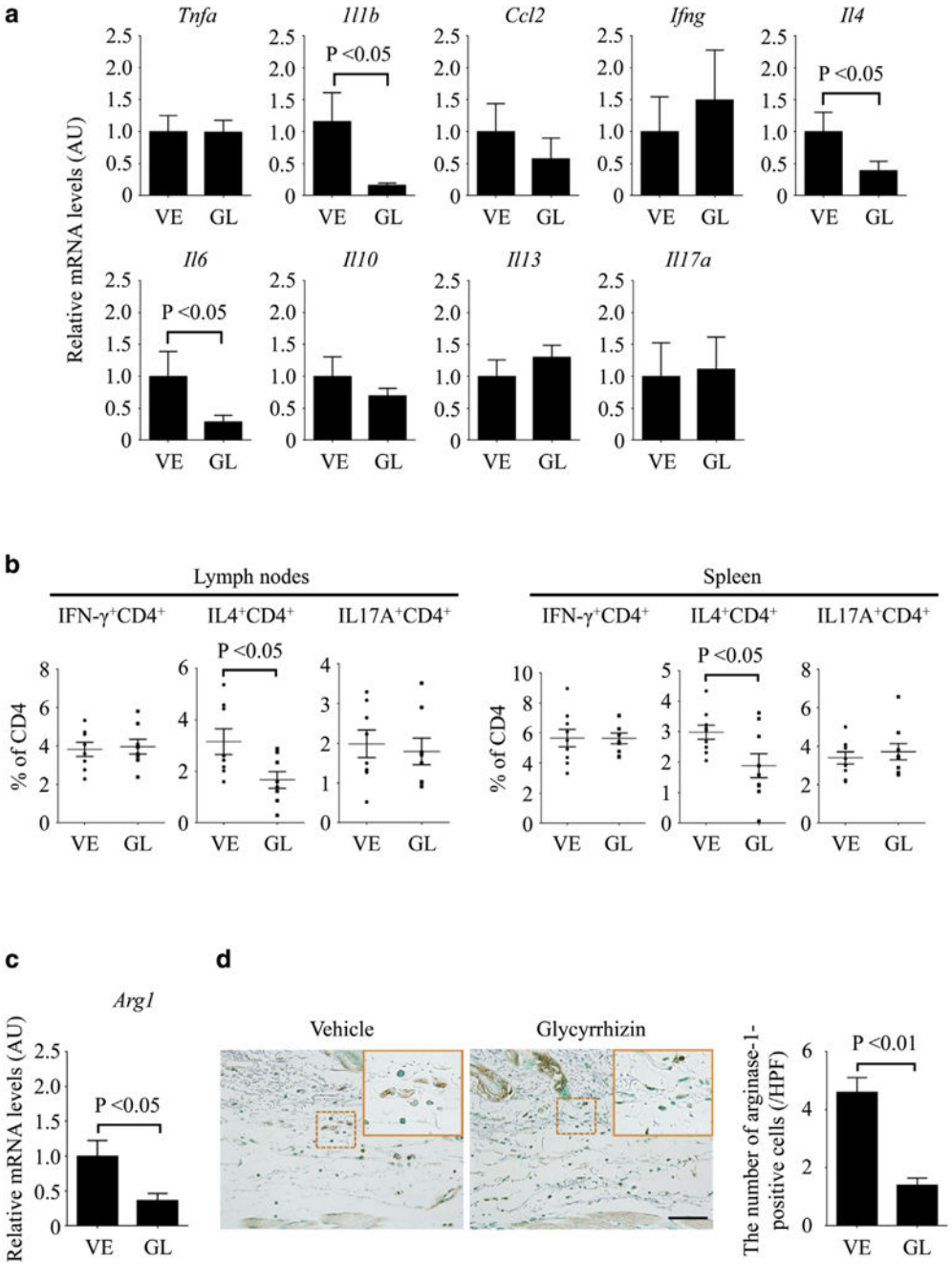

Figure 3. Glycyrrhizin alleviates the induction of Th2-skewed immune polarization and M2 macrophage differentiation in BLM-treated mice

(**a–d**) Mice were subcutaneously injected with BLM or PBS along with the administration of glycyrrhizin (GL) or PBS (vehicle [VE]). (**a**) *Tnfa*, *Il1b*, *Ccl2*, *Ifng*, *Il4*, *Il6*, *Il10*, *Il13*, and *Il17a* mRNA levels in the lesional skin were measured by quantitative real-time reverse transcription–PCR. (**b**) The proportions of IFN-γ–, IL-4–, and IL-17A–producing $CD4^+$ T cells were evaluated by flow cytometry with lymphocytes isolated from skin-draining lymph nodes and spleen. (**c**) mRNA expression of the *Arg1* gene and (**d**) the number of arginase-1–positive cells were evaluated in the lesional skin by quantitative real-time reverse

transcription–PCR and by immunohistochemistry, respectively. The insets depict representative inflammatory cells shown with dotted squares. Each graph represents mean ± standard error of the mean of the indicated parameters (n = 8–9 per each group in **a**, **b**, and **c**). Representative images are shown for immunohistochemistry (n = 5). Scale bar = 20 μm. AU, arbitrary unit; BLM, bleomycin; GL, glycyrrhizin; HPF, high power field; PBS, phosphate buffered saline; Th, T helper; VE, vehicle.

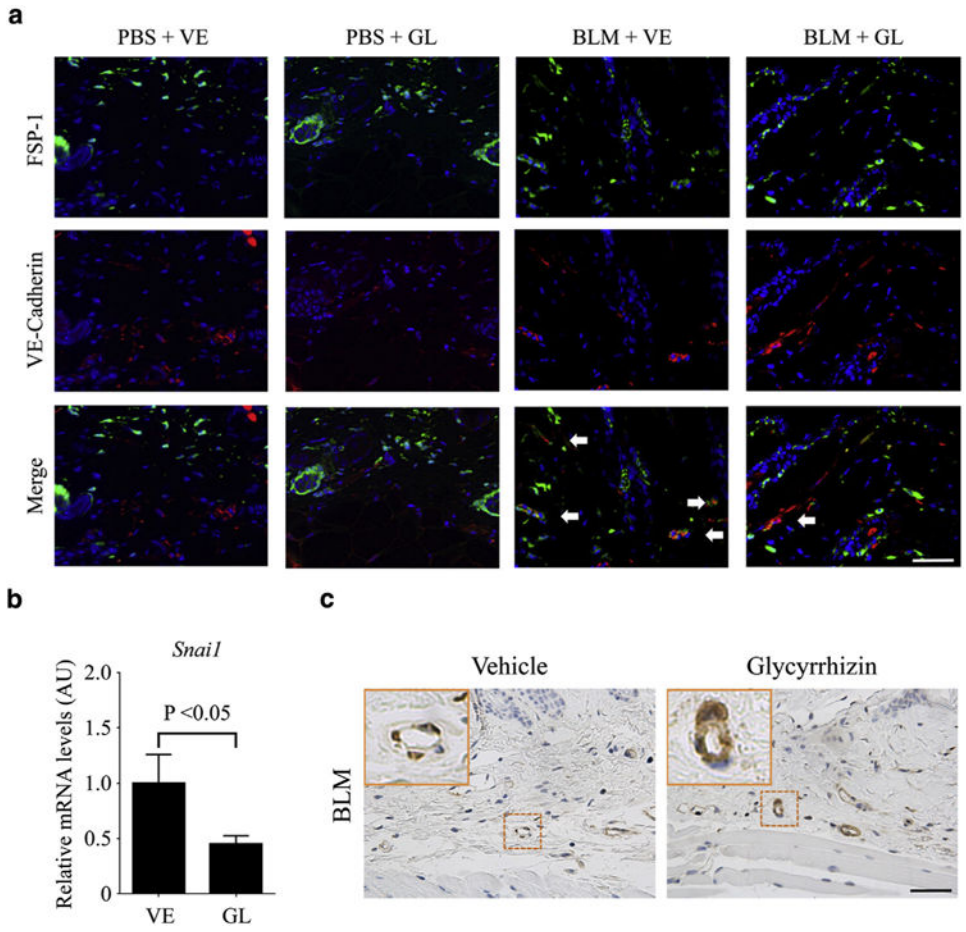

Figure 4. Glycyrrhizin abrogates the induction of EndoMT in BLM-treated mice

(**a**) Immunofluorescence staining of FSP-1 (green) and VE-cadherin (red) in skin samples from PBS- or BLM-treated mice with the administration of glycyrrhizin (GL) or PBS (vehicle [VE]). FSP-1/VE-cadherin double-positive cells were indicated with arrows. The number of FSP-1/VE-cadherin double-positive cells was counted under magnification × 200 (n = 4). (**b**) mRNA expression of the *Snail1* gene was determined by quantitative real-time reverse transcription–PCR in the lesional skin of BLM-treated mice exposed to glycyrrhizin or not. Values are the means ± standard error of the mean (n = 6). (**c**) Skin sections were stained for α-SMA. α-SMA–positive cells in vascular walls were recognized as pericytes. Representative images of immunohistochemistry are shown (n = 6). The insets depict representative blood vessels shown with dotted squares. Scale bars = 20 μm. α-SMA, α-smooth muscle actin; AU, arbitrary unit; BLM, bleomycin; EndoMT, endothelial-to-mesenchymal transition; FSP-1, fibroblast-specific protein-1; GL, glycyrrhizin; PBS, phosphate buffered saline; VE, vehicle; VE-Cadherin, vascular endothelial cadherin.

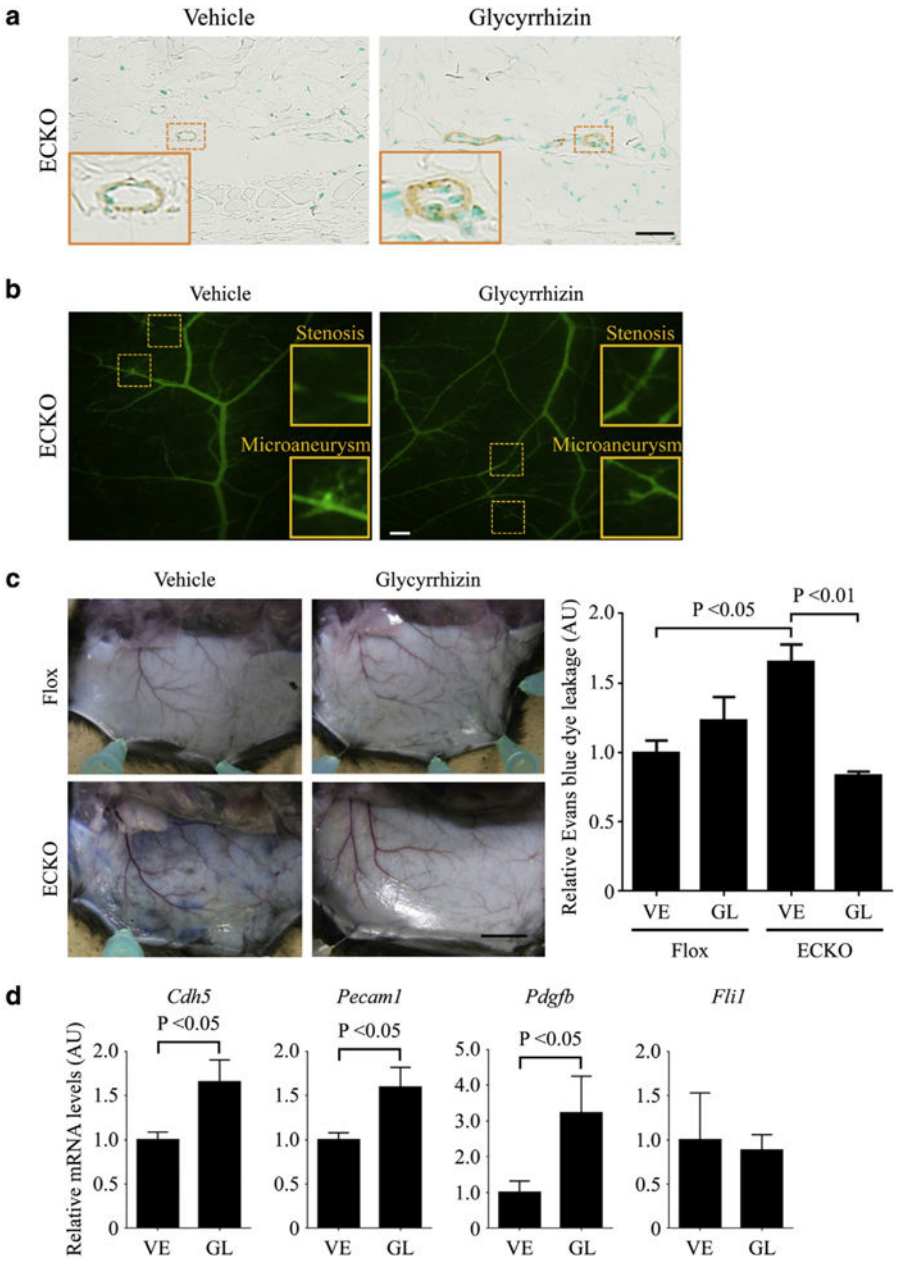

Figure 5. Glycyrrhizin improves the leaky vascular phenotype of *Fli1* ECKO mice

(**a**–**d**) *Fli1* ECKO mice were administered glycyrrhizin (GL) or PBS (vehicle [VE]) for 2 weeks. (**a**) The degree of pericyte coverage was evaluated by immunostaining for α-SMA in dermal small vessels of these mice (n = 5). Vascular structure and vascular permeability were assessed by (**b**) fluorescein isothiocyanate-dextran injection (n = 5) and (**c**) Evans blue dye injection (n = 6), respectively. The graph in **c** represents quantification of Evans blue dye extravasation by formamide extraction. (**d**) *Cdh5*, *Pecam1*, *Pdgfb*, and *Fli1* mRNAs were determined by quantitative real-time reverse transcription–PCR in the skin of these mice (n = 6). Each graph represents mean ± standard error of the mean of the indicated parameters. The insets depict representative blood vessels in (**a**) and vascular stenosis and microaneurysm in (**b**), which are shown with dotted squares. Scale bars = 20 μm for **a**, 200

μm for **b**, and 1 cm for **c**. α-SMA, α-smooth muscle actin; AU, arbitrary unit; ECKO, endothelial cell-specific *Fli1* knockout; GL, glycyrrhizin; PBS, phosphate buffered saline; VE, vehicle.